Available online at www.sciencedirect.com
SCIENCE DIRECT
Polymer 46 (2005) 11837–11843
polymer
www.elsevier.com/locate/polymer

Correlation between crystallization kinetics and melt phase behavior of crystalline–amorphous block copolymer/homopolymer blends

Jen-Yung Hsu [a], Bhanu Nandan [a], Mei-Chun Chen [a], Fang-Choyu Chiu [b], Hsin-Lung Chen [a,*]

[a] *Department of Chemical Engineering, National Tsing Hua University, Hsin-Chu 30013, Taiwan, ROC*
[b] *Department of Chemical and Materials Engineering, Chang Gung University, Kwei-San, Taoyuan 333, Taiwan, ROC*

Received 22 March 2005; received in revised form 12 September 2005; accepted 10 October 2005
Available online 28 October 2005

Abstract

We show that the phase behavior of the strongly segregated blend consisting of a crystalline–amorphous diblock copolymer (C-*b*-A) and an amorphous homopolymer (h-A), which depends on the degree of wetting of A blocks by h-A, can be probed by the crystallization kinetics of the C block. A lamellae-forming poly(ethylene oxide)-*block*-polybutadiene (PEO-*b*-PB) was blended with PB homopolymers (h-PB) of different molecular weights to yield the blends exhibiting 'wet brush', 'partially dry brush', and 'dry brush' phase behavior in the melt state. The crystallization rate of the PEO blocks upon subsequent cooling, as manifested by the freezing (crystallization) temperature (T_f), was highly sensitive to the morphology and spatial connectivity of the microdomains governed by the degree of wetting of PB blocks. As the weight fraction of h-PB reached 0.48, for instance, T_f experienced an abrupt rise as the system entered from the wet-brush to the dry-brush regime, because the crystallization in the PEO cylindrical domains in the former required very large undercooling due to a homogeneous nucleation-controlled mechanism while the process could occur at the normal undercooling in the latter since PEO domains retained lamellar identity with extended spatial connectivity. Our results demonstrate that as long as the C block is present as the minor constituent the melt phase behavior of C-*b*-A/h-A blends can also be probed using a simple cooling experiment operated under differential scanning calorimetry (DSC).

Keywords: Crystallization kinetics; Block copolymer blends; Melt phase behavior

1. Introduction

Molecular self-assembly in diblock copolymers (A-*b*-B) can generate a variety of long-range ordered microdomains, including one-dimensionally (1D) stacked lamellae, gyroids, hexagonally packed cylinders and body-center cubic (BCC) packed spheres, depending upon the strength of interblock repulsion and the volume fractions of the constituting blocks (f_A) [1]. Since the domain structure is closely governed by f_A, block copolymer mesophase may also be tailored by blending A-*b*-B with homopolymer A (h-A) [1–10]. The phase behavior of A-*b*-B/h-A blends is governed not only by the segregation strength and f_A but also by the molecular weight of h-A ($M_{h\text{-}A}$) relative to that of A blocks ($M_{b\text{-}A}$), which is expressed by the factor $\alpha = M_{h\text{-}A}/M_{b\text{-}A}$. The magnitude of α dictates the degree of wetting of A block emanating from the domain interface by h-A, or in other words, the degree of mixing between h-A chains and A block chains [3,5,7,8].

h-A chains dissolve and distribute uniformly in A microdomains to swell the distance between the junction points at the domain interface when $M_{h\text{-}A}$ is obviously smaller than $M_{b\text{-}A}$, i.e. $\alpha < 1$. This case is known as the 'wet brush' [3,5] . Under the constraint of melt incompressibility, the effective wetting of A blocks by h-A causes stretchings and hence entropic losses of these chains. If both A and B blocks form lamellar microdomains prior to the addition of h-A, the free energy penalty can be released by introducing curvature to the interface, i.e. by changing the morphology of B domain from lamellae with zero interfacial curvature to cylinder or sphere [5]. Consequently, a series of domain structure transformation from lamellae to cylinder to sphere can occur with increasing h-A composition in the wet-brush regime.

When $M_{h\text{-}A}$ is approximately the same as $M_{b\text{-}A}$, i.e. $\alpha \approx 1$, a 'dry-brush' kind of phase behavior is obtained [3,5,9,10]. In this case, h-A chains still enter into A domains but they remain unmixed with A blocks due to high conformational entropy penalty and are hence localized to the mid-regions of the domains leaving the junction point separation unchanged.

* Corresponding author. Tel.: +886 3 572 1714; fax: +886 3 571 5408.
E-mail address: hslchen@mx.nthu.edu.tw (H.-L. Chen).

0032-3861/$ - see front matter © 2005 Elsevier Ltd. All rights reserved.
doi:10.1016/j.polymer.2005.10.054

In the dry-brush blend of lamellae-forming A-*b*-B and h-A, the thickness of A domain is swollen continuously with increasing h-A composition while retaining the lamellar identity and thickness of B domain. B lamellae may, however, become highly isolated at high h-A composition, leading to the formation of cylindrical or spherical vesicles [9–11].

The phase behavior of A-*b*-B/h-A blends can be revealed by studying the effect of h-A composition on the morphology of B microdomain using techniques such as small angle X-ray scattering (SAXS) and transmission electron microscopy (TEM). Wet-brush blending will induce transformation of domain morphology at certain h-A compositions, whereas the domain structure remains the same with respect to h-A composition in the dry-brush system. In the present study, we intend to demonstrate that if one of the blocks becomes crystallizable, the phase behavior of the blend may also be probed by the corresponding crystallization kinetics using differential scanning calorimetry (DSC). This approach may effectively complement SAXS and TEM for characterizing the morphology of the blend and the extent of homopolymer solubilization in the blend.

Our central idea lies in the fact that the crystallization kinetics of the crystalline block (denoted by 'C' block) in crystalline–amorphous (C–A) diblock systems is strongly affected by the morphology of the microdomains formed by C blocks [12–20]. In recent works, we have systematically investigated the crystallization behavior of poly(ethylene oxide) (PEO) block in the poly(ethylele oxide)-*block*-polybutadiene (PEO-*b*-PB)/h-PB blends with respect to the change of h-PB composition [12–14]. For the wet-brush blend in which the PEO domains underwent lamellae → cylinder → sphere transition with increasing h-PB composition [12,13], the freezing (crystallization) temperature (T_f) of PEO block determined from the fixed cooling rate experiment in a DSC experienced distinct transitions at the compositions corresponding to the morphological transformations. The undercoolings required to initiate crystallizations in cylindrical and spherical microdomains were found to be much larger than that associated with the lamellar melt due to a homogeneous nucleation-controlled mechanism [21,22]. For the dry-brush system in which the lamellar identity of PEO domain was retained [14], crystallization could take place at the normal undercooling (i.e. the undercooling comparable to that associated with h-PEO) except at very high h-PB compositions where PEO lamellae became highly isolated and hence formed spherical vesicles. Because the spherical vesicles considerably outnumbered the heterogeneous nuclei, the crystallization of PEO blocks within most vesicle had to proceed through homogeneous nucleation which required very deep undercooling [14,19].

These previous findings attest that once C block is present as the minor constituent in C-*b*-A/h-A blend, its crystallization kinetics (manifested by the magnitude of T_f) is directly related to the morphology and spatial connectivity of the microdomains governed by the degree of wetting of A blocks by h-A. Consequently, the phase behavior of the diblock blends may be probed by measuring the T_f of C block upon cooling from the melt state. The feasibility of this approach will be demonstrated here using PEO-*b*-PB/h-PB blend as the model system. In the present study, a lamellae-forming PEO-*b*-PB is blended with h-PB of different molecular weights to yield the blends exhibiting wet-brush, partial dry-brush and dry-brush phase behavior in the melt state. In contrast to our previous studies concerning the dependence of T_f on h-PB composition under a fixed $M_{h\text{-}PB}$, here we will center on the variation of T_f along the $M_{h\text{-}PB}$ coordinate at a given blend composition.

2. Experimental section

2.1. Materials and blend preparation

PEO-*b*-PB with a polydispersity index (M_w/M_n) of 1.04 was synthesized by sequential anionic polymerization of butadiene and ethylene oxide (Polymer Source, Inc.). M_n of the PEO and PB block was $M_{b\text{-}PEO}=7500$ and $M_{b\text{-}PB}=5500$, respectively, which prescribed the volume fraction of PB (f_{PB}) = 0.46. A series of 1,4-addition h-PB with $M_{h\text{-}PB}=900$, 2300, 4500, 6000 and 8800 was used for blending with PEO-*b*-PB. These samples were designated as h-PB0.9K, h-PB2K, h-PB4K, h-PB6K and h-PB9K with the values of α ($=M_{h\text{-}PB}/M_{b\text{-}PB}$) of 0.16, 0.42, 0.81, 1.1 and 1.6, respectively. Each blend was prepared by solution mixing using toluene as the co-solvent, followed by removing the solvent in vacuo at 80 °C. The blend compositions are expressed in terms of the weight fraction of h-PB in the blend, $w_{h\text{-}PB}$.

2.2. SAXS measurement

SAXS was utilized to probe the morphology of PEO microdomains in the melt state. All SAXS measurements were performed at 70 °C ($T_{m,PEO} < 70\ °C < T_{ODT}$) to avoid the effect of PEO crystallization. Details of the SAXS setup have been described elsewhere [13]. In brief, the SAXS apparatus consisted of an 18 kW rotating-anode X-ray generator operated at 40 kV × 200 mA (Rigaku), a graphite crystal for incident monochromatization, and a two-dimensional position-sensitive detector (ORDELA model 2201X, Oak Ridge Detector Laboratory Inc.). The intensity profiles were output as the plot of scattering intensity (I) vs. scattering vector, $q=(4\pi/\lambda)\sin(\theta/2)$ (θ = scattering angle).

2.3. DSC measurement

T_f of the PEO blocks in the blend was measured by a fixed cooling rate experiment in a TA Instrument 2000 DSC equipped with the RCS cooling system. The sample was first annealed at 85 °C for 5 min and then cooled to −50 °C at a rate of 5 °C/min for recording the crystallization exotherm. The temperature corresponding to the exothermic peak was defined as T_f of the sample.

3. Results and discussions

3.1. PEO microdomain morphology in the melt state

The morphology of PEO microdomain in the melt state was first probed using SAXS to verify that different degrees of mixing between PB block and h-PB are accessible in the blends studied here. In the wet-brush blend, PEO domain is expected to undergo a transformation from lamellae to cylinder to sphere with increasing $w_{h\text{-}PB}$, whereas its lamellar identity is expected to retain in the dry-brush system. Fig. 1(a) shows the SAXS profiles of PEO-*b*-PB/h-PB0.9K blends ($\alpha = 0.16$) in the melt state. Neat PEO-*b*-PB displays well-defined lattice peaks with relative positions (1:2:3:4:5) closely relevant to 1D stacked lamellar morphology. The interlamellar distance calculated from the primary peak position ($L = 2\pi/q_m$) is 21.0 nm. The thickness of PEO lamellae is, therefore, 11.3 nm considering that the volume fraction of PEO in the blend is 0.54.

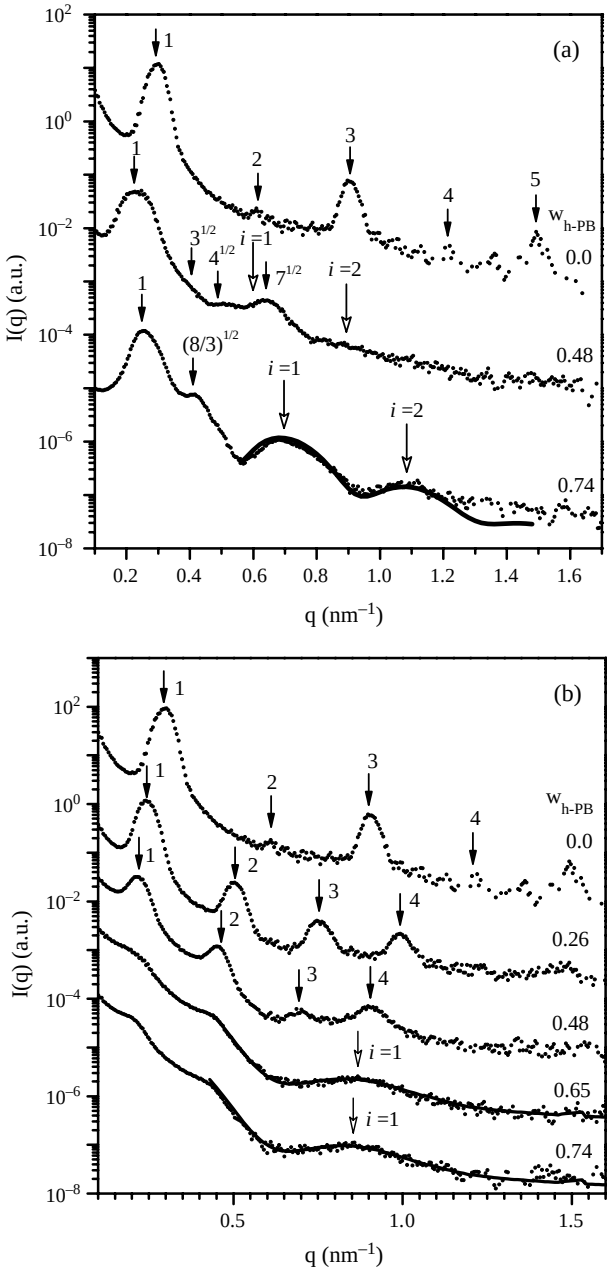

Fig. 1. SAXS profiles of (a) PEO-*b*-PB/h-PB0.9K ($\alpha = 0.16$) and (b) PEO-*b*-PB/h-PB6K ($\alpha = 1.1$) blends in the melt state. The SAXS experiments were conducted at 70 °C. The lattice peaks are marked by solid arrows, whereas the maxima denoted by '$i = n$' ($n = 1, 2$) are the form factor peaks associated with scattering from individual microdomains. In (a), the solid curve displays the fitting result of the observed form factor profile using the theoretical form factor of polydisperse spheres with the mean radius of 8.4 nm. The solid curves in (b) are the profiles calculated using theoretical lamellar form factor with the average lamellar thickness of 10.6 nm. Gaussian distributions were assumed for the domain size.

As $w_{h\text{-}PB}$ increases to 0.48, the SAXS profile of the blend shows lattice peaks with the relative positions of $1{:}3^{1/2}{:}4^{1/2}{:}7^{1/2}$, indicating that the structure has transformed into hexagonally packed cylinders. Two broad maxima marked by '$i = n$' ($n = 1$, 2) are attributed to the form factor scattering of the individual cylindrical microdomains. The average radius of the cylinders estimated from the position of the first-order form factor maximum ($q_m^{i=1}$) via $R = 4.98/q_m^{i=1}$ is 8.5 nm [5]. As $w_{h\text{-}PB}$ is further increased to 0.74, the scattering profile is characterized by two lattice peak with the relative position of $1{:}(8/3)^{1/2}$ along with two form factor maxima. This scattering pattern corresponds to the morphology of face-centered cubic (FCC) packed PEO spheres [23]. Although sphere is the equilibrium morphology for the individual PEO domain at this composition, the observed FCC packing is metastable as it was formed during the solvent evaporation process and somehow trapped into the bulk after complete solvent removal. Upon heating this metastable FCC phase transformed to BCC phase at ca. 200 °C but the BCC packing underwent another transition into an equilibrium FCC phase above 220 °C [24]. The solid curve in Fig. 1(a) displays the fitting result of the observed form factor profile using the theoretical form factor of polydisperse spheres with the assumption of Gaussian distribution of radius [25]. The mean radius of the spherical microdomains deduced from the fit is 8.4 nm. The SAXS pattern in Fig. 1(a) clearly demonstrates the transformation of melt morphology from lamellae to cylinder to sphere, and hence verifies that PEO-*b*-PB/h-PB0.9K blend is a wet-brush system in which h-PB is homogenously solublized in the PB microdomains. Table 1 summarizes the microdomain morphology and the morphological parameters of the blend.

On increasing $M_{h\text{-}PB}$ to 4500 ($\alpha = 0.42$), a similar morphological transformation to that found in PEO-*b*-PB/h-PB0.9K was observed with increasing $w_{h\text{-}PB}$. The composition dependence of the melt morphology of this blend system is also tabulated in Table 1. The lamellae-to-cylinder transition was found to occur near $w_{h\text{-}PB} = 0.57$ (compared with $w_{h\text{-}PB} = 0.48$ in PEO-*b*-PB/h-PB0.9K system), indicating that the morphological transformation gets delayed as α increases from 0.16 to 0.42. This shows that the higher molecular weight h-PB no longer mixed homogeneously with the PB blocks in the PB phase. Hence PEO-*b*-PB/h-PB4.5K blend is described as a 'partially dry brush' system.

Table 1
The microdomain morphology and the morphological parameters of the PEO-*b*-PB/h-PB blends in the melt state

$M_{h\text{-}PB}$	$w_{h\text{-}PB}$	D (nm)[a]	l_{PEO} (nm)[b]	R (nm)[c]	PEO domain morphology
Neat diblock	0.0	21.0	11.3		Lamellae
900	0.26	24.2	9.7		Lamellae
900	0.31	25.1	9.1		Lamellae
900	0.40	28.0		8.1	Cylinder
900	0.48	32.1		8.5	Cylinder
900	0.57	32.1		8.4	Cylinder
900	0.65	41.5		8.8	Sphere
900	0.74	43.2		8.4	Sphere
4500	0.26	25.5	10.2		Lamellae
4500	0.31	25.6	9.5		Lamellae
4500	0.40	32.8	9.8		Lamellae
4500	0.48	35.7	9.6		Lamellae
4500	0.57	48.5		9.5	Cylinder
4500	0.65	47.6		9.7	Cylinder
4500	0.74	47.8		9.6	Sphere
6000	0.31	26.2	9.7		Lamellae
6000	0.40	28.9	9.5		Lamellae
6000	0.48	31.9	8.6		Lamellae
6000	0.57		10.3[d]		Lamellae
6000	0.65		10.6[d]		Lamellae
6000	0.74		10.6[d]		Lamellae

[a] D is the interdomain distance calculated from the primary peak position ($D=2\pi/q_m$).
[b] l_{PEO} is the thickness of PEO lamellae ($l_{PEO}=D\times f_{PEO}$; f_{PEO} is the overall volume fraction of PEO).
[c] R is the mean radius of cylinders or spheres calculated from the observed form factor profiles.
[d] Obtained from the fits of the observed form factor by the theoretical lamellar form factor.

When $M_{h\text{-}PB}$ was further increased to 6000 ($\alpha=1.1$), PEO microdomain does not undergo any morphological transformation as manifested from the SAXS profiles in Fig. 1(b). The blends are found to exhibit lamellar diffraction peaks up to $w_{h\text{-}PB}=0.48$, indicating the presence of long-range ordered lamellar arrays. These lattice peaks vanish when $w_{h\text{-}PB}>0.57$, where the corresponding SAXS profiles are replaced by a broad form factor peak which is fittable by the theoretical lamellar form factor assuming Gaussian distribution of the lamellar thickness (cf. the solid curves in Fig. 1(b)) [9]. The average thickness of the PEO lamellae deduced from the fit is 10.6 nm, which agrees reasonably with the value of 11.3 nm calculated from the interlamellar distance of the neat diblock. Therefore, the lamellar identity and thickness of PEO microdomains are essentially unperturbed upon blending, a typical feature of dry-brush blend. The dominance of the scattering pattern by the form factor profile at large $w_{h\text{-}PB}$ attests that the PEO lamellae become highly isolated, forming cylindrical or spherical vesicles dispersed in the PB matrix. The result is consistent with our previous study on the dry-brush PEO-*b*-PB/h-PB blend with different molecular weight combination [14].

The SAXS results have hence verified that different degrees of wetting of the PB blocks, ranging from wet-brush to partially dry-brush to dry-brush, are accessible in the blends under study. The crystallization kinetics of the PEO blocks in these blends are hence investigated to demonstrate the feasibility of probing the melt phase behavior of C-*b*-A/h-A blends by measuring the T_f of C block upon cooling from the melt.

3.2. Crystallization kinetics and its correlation with melt phase behavior

It has been observed in our previous studies that the crystallization kinetics exhibited a distinct correlation with the microdomain morphology in the wet-brush PEO-*b*-PB/h-PB blends [12,13]. In the lamellar melt, crystallization occurred through a series of heterogeneous nucleation followed by long-range crystal growth such that the process could be initiated and completed at the normal undercoolings. A very deep undercooling was, however, required to initiate the homogeneous nucleation in most cylindrical and spherical microdomains because the microdomains outnumbered the heterogeneous nuclei significantly. In the dry-brush system, since lamellar structure was retained over the whole composition range, heterogeneous nucleation coupled with long-range crystal growth was observed except at very high $w_{h\text{-}PB}$ where isolated vesicles were formed [14].

Here, we present the crystallization kinetics of the PEO blocks as a function of $M_{h\text{-}PB}$ for a series of blend compositions. Figs. 3–5 display the DSC cooling curves of the blends with the compositions of $w_{h\text{-}PB}=0.26$, 0.48, and 0.74. The corresponding T_f (i.e. peak temperature of the crystallization exotherm) is plotted as a function of $M_{h\text{-}PB}$ on a semi-logarithmic scale in the inset of each figure. All the blend

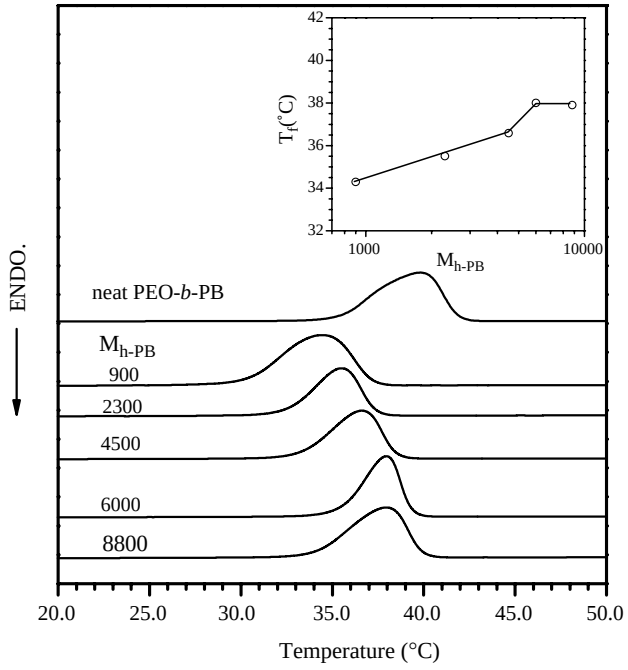

Fig. 2. DSC cooling profiles of PEO-*b*-PB/h-PB blends with $w_{h\text{-}PB}=0.26$. $M_{h\text{-}PB}$ is indicated in the figure. The inset shows the corresponding freezing temperature (T_f) vs. $M_{h\text{-}PB}$ plot.

systems with $w_{h\text{-}PB}=0.6$ show a T_f around 34∼40 °C (cf. Fig. 2). According to the morphological characterization discussed previously, PEO blocks in these blends self-assemble into well-stacked lamellar domains in the melt state irrespective of the degree of wetting of the PB blocks. Due to the extended spatial connectivity of these lamellar domains, crystal growth can propagate over macroscopic length scale from the heterogeneous nuclei formed at the normal undercoolings. T_f is found to increase progressively with increasing $M_{h\text{-}PB}$ in the wet-brush and partially dry-brush regime (i.e. $M_{h\text{-}PB}\leq 4500$) but it experiences a sudden yet small rise as the system enters the dry-brush regime. This sudden increase of T_f reveals the sensitivity of the crystallization kinetics to the phase behavior of the blend as to whether PB blocks are wetted by h-PB, but the sensitivity is not high for the cases where the PEO blocks form well-stacked lamellar domains irrespective of $M_{h\text{-}PB}$.

Dependence of T_f on $M_{h\text{-}PB}$ becomes much more dramatic when $w_{h\text{-}PB}$ is increased to 0.48, as shown in Fig. 3. The crystallizations in the wet-brush blends ($M_{h\text{-}PB}<4500$) in which PEO blocks form cylindrical microdomains occur at a very deep undercooling ($T_f\approx -29$ °C) due to a homogeneous nucleation-controlled mechanism. T_f rises slightly to −24 °C as $M_{h\text{-}PB}$ is increased to 4500 where the blend becomes a partially dry-brush system. Although PEO blocks in this blend form lamellar domains in the melt state (cf. Table 1); these domains are in the form of isolated vesicles such that the crystallization in most of these vesicles still has to proceed through homogeneous nucleation. The rate of homogeneous nucleation is proportional to the volume of the domains in which it takes place; therefore, the vesicles exhibit a higher T_f since the average volume per vesicle is larger than that of the individual cylindrical microdomains in the corresponding wet-brush blends. A large abrupt jump of T_f to ca. 33 °C is observed as the system enters the dry-brush regime in which the PEO domains not only retain their lamellar identity but also form regular stacks (cf. Fig. 1(b)). In this case, PEO crystallization can take place at the normal undercoolings due to the extended spatial connectivity of the lamellar domains. Fig. 5 clearly shows the distinct correlation between the crystallization kinetics and the melt phase behavior of PEO-*b*-PB/h-PB blends. Using T_f to probe the degree of wetting of PB blocks is hence particularly feasible at this composition.

When $w_{h\text{-}PB}$ is further increased to 0.74 where PEO blocks form spherical microdomains in the wet-brush blends, an even higher undercooling ($T_f\approx -35$ °C) is required for the crystallization (compared with that associated with the cylinder-forming wet-brush blends) owing to smaller volume of the individual sphere (cf. Fig. 4). T_f is found to increase to ca. −28 °C as $M_{h\text{-}PB}$ is increased to 4500 where the PEO domains are cylinders. T_f experiences an abrupt jump to −22 °C as the system enters the dry-brush regime, but the rise is much less significant than that found for $w_{h\text{-}PB}=0.48$. Now the PEO blocks in the dry-brush blends require very large undercooling to crystallize even though they form lamellar domains in the melt as ascertained from the SAXS results. This can be explained by the fact that these lamellae are in the form of vesicles with limited spatial connectivity, as also supported by the corresponding SAXS results in Fig. 1(b).

In Fig. 5, T_f is plotted as a function of α for the three compositions to summarize the dependence of crystallization kinetics on the phase behavior of PEO-*b*-PB/h-PB blends in the melt state. $\alpha=1$ approximately specifies the borderline

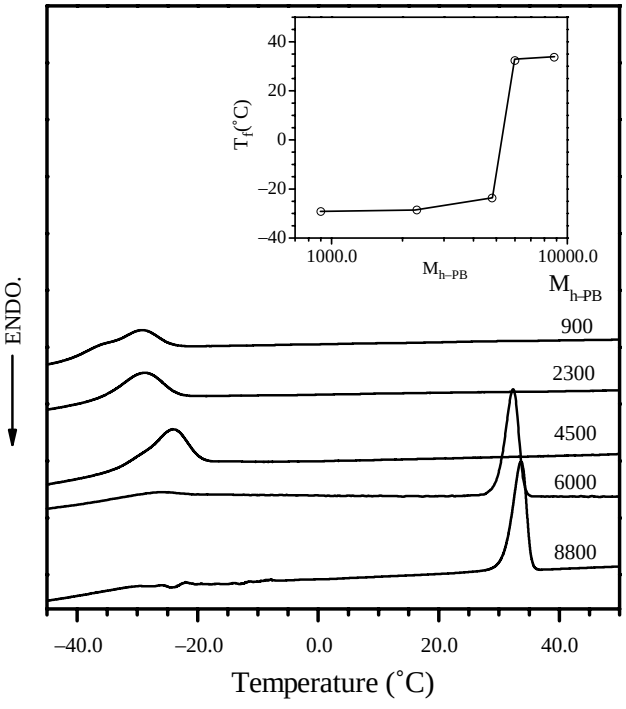

Fig. 3. DSC cooling profiles of PEO-*b*-PB/h-PB blends with $w_{h\text{-}PB}=0.48$. $M_{h\text{-}PB}$ is indicated in the figure. The inset shows the corresponding freezing temperature (T_f) vs. $M_{h\text{-}PB}$ plot.

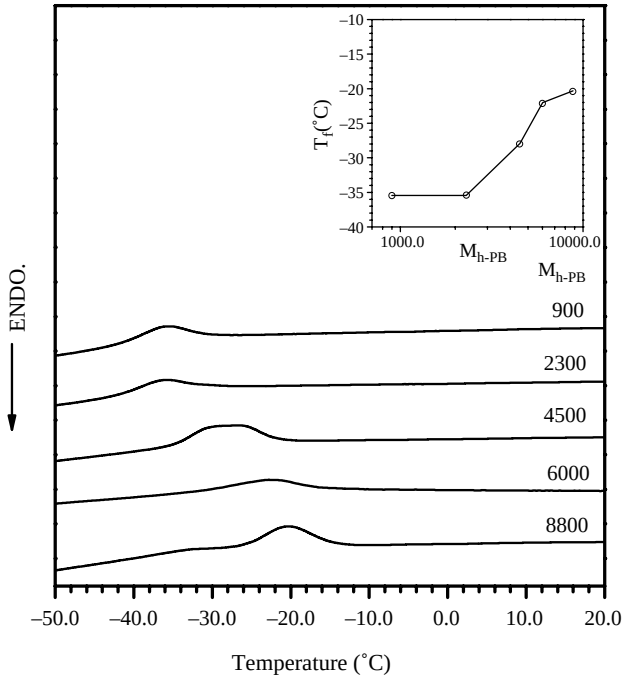

Fig. 4. DSC cooling profiles of PEO-*b*-PB/h-PB blends with $w_{h\text{-}PB}=0.74$. $M_{h\text{-}PB}$ is indicated in the figure. The inset shows the corresponding freezing temperature (T_f) vs. $M_{h\text{-}PB}$ plot.

beyond which the dry-brush behavior is accessed. A distinct correlation between the crystallization kinetics and the degree of wetting of PB blocks by h-PB is revealed in the figure, particularly for $w_{h\text{-}PB}=0.48$ and 0.74. Under the prescribed block length and cooling rate (i.e. −5 °C/min), T_f generally situates at around 34∼40 °C when PEO blocks form well-stacked lamellar domains; it drops down to −22 to −24 °C when the lamellar domains are in the form of isolated vesicles. T_f decreases further to −29 and −35 °C in the cases of cylindrical and spherical microdomains, respectively. The dependence of T_f on α thus provides an alternative to qualitatively probe the extent of mixing between A blocks and h-A in C-*b*-A/h-A blends as long as the C block is present as the minor constituent.

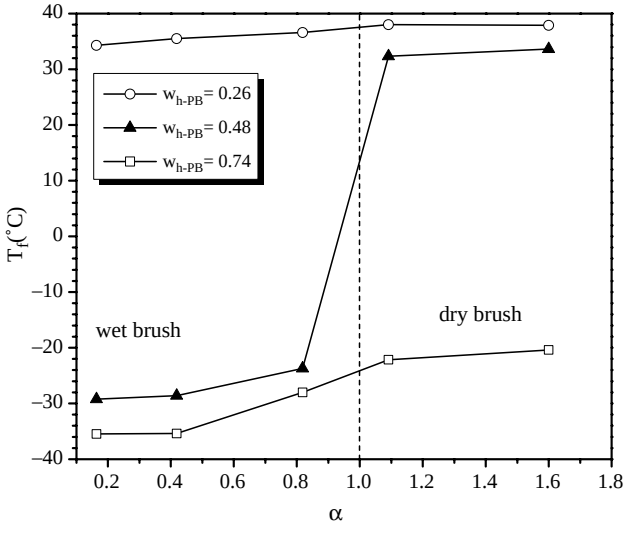

Fig. 5. T_f as a function of α for the three compositions of PEO-*b*-PB/h-PB blends to summarize the dependence of crystallization kinetics on the phase behavior of the blends in the melt state. $\alpha=1$ approximately specifies the borderline beyond which the dry-brush behavior is accessed. A distinct correlation between the crystallization kinetics and the degree of wetting of PB blocks by h-PB is revealed in the figure, particularly for $w_{h\text{-}PB}=0.48$ and 0.74.

4. Conclusions

Using PEO-*b*-PB/h-PB as the model system, we have revealed the feasibility of probing the melt phase behavior of C-*b*-A/h-A blends using the freezing (crystallization) temperature obtained from a standard DSC cooling experiment. This approach relies on the fact that the overall crystallization kinetics of C block is highly sensitive to the morphology and spatial connectivity of C microdomains, which are governed by the degree of wetting of A block and $w_{h\text{-}A}$. The dependence of T_f on the melt phase behavior is particularly evident at relatively high $w_{h\text{-}A}$ where C blocks in the wet-brush blends form highly discrete domains such as cylinders or spheres but those in the corresponding dry-brush system self-organize into lamellae with extended spatial connectivity. In this case, the crystallizations in the former have to be initiated at very large undercooling due to a homogeneous nucleation-controlled mechanism, whereas in the later the process can take place at the normal undercooling because the crystal growth can propagate over macroscopic length scale from the heterogeneous nuclei. Consequently, T_f will exhibit a large abrupt rise as the system enters from the wet-brush (with homogeneous nucleation-controlled) to the dry-brush regime (with heterogeneoius nucleation coupled with long-range crystal growth).

Acknowledgements

This work was supported by the National Science Council of Taiwan under grant No. NSC 93-2216-E-007-011.

References

[1] Hamley IW. The physics of block copolymers. Oxford: Oxford University Press; 1998.
[2] Roe RJ, Zin WC. Macromolecules 1984;17:189.
[3] Hashimoto T, Tanaka H, Hasegawa H. Macromolecules 1990;23:4378.
[4] Nojima S, Roe RJ, Rigby D, Han CC. Macromolecules 1990;23:4305.
[5] Tanaka H, Hasegawa H, Hashimoto T. Macromolecules 1991;24:240.
[6] Winey KI, Thomas EL, Fetters LJ. Macromolecules 1992;25:2645.
[7] Matsen MW. Macromolecules 1995;28:5765.
[8] Matsen MW. Phys Rev Lett 1995;74:4225.
[9] Koizumi S, Hasegawa H, Hashimoto T. Makromol Chem, Macromol Symp 1992;62:75.
[10] Hashimoto T, Koizumi S, Hasegawa H. Physica B 1995;213:676.
[11] Kinning D, Winey KI, Thomas EL. Macromolecules 1988;21:3502.
[12] Chen HL, Hsiao SC, Lin TL, Yamauchi K, Hasegawa H, Hashimoto T. Macromolecules 2001;34:671.

[13] Chen HL, Wu JC, Lin TL, Lin JS. Macromolecules 2001;34:6936.
[14] Chen HL, Lin SY, Huang YY, Chiu FC, Liou W, Lin JS. Macromolecules 2002;35:9434.
[15] Loo YL, Register RA, Ryan AJ, Dee GT. Macromolecules 2001;34: 8968.
[16] Xu JT, Turner SC, Fairclough JPA, Mai SM, Ryan AJ. Macromolecules 2002;35:3614.
[17] Loo YL, Register RA, Ryan AJ. Macromolecules 2002;35:2365.
[18] Loo YL, Register RA, Ryan AJ. Phys Rev Lett 2000;84:4120.
[19] Muller AJ, Balsamo V, Arnal ML, Jakob T, Schmalz H, Abetz V. Macromolecules 2002;35:3048.
[20] Zhu L, Cheng SZD, Calhoun BH, Ge Q, Quirk RP, Thomas EL, et al. Polymer 2001;42:5829.
[21] Turnbull D, Cormia RL. J Chem Phys 1961;34:820.
[22] Cormia RL, Price FP, Turnbull D. J Chem Phys 1962;37:1333.
[23] Huang YY, Chen HL, Hashimoto T. Macromolecules 2003;36:764.
[24] Huang YY. PhD Thesis, National Tsing Hua University; 2004.
[25] Hashimoto T, Fujimura M, Kawai H. Macromolecules 1980;13:1660.